# General Synthesis of Iron(III) Tetrathiolate Complexes. Structural and Spectroscopic Models for the [Fe(Cys-*S*)$_4$] Center in Oxidized Rubredoxin

**Lynn E. Maelia, Michelle Millar,* and Stephen A. Koch***

Department of Chemistry, State University of New York at Stony Brook, Stony Brook, New York 11794-3400

*Received June 9, 1992*

A general synthetic route to stable $[Fe^{III}(SR)_4]^-$ complexes is described. The reaction of DMF solutions of $[R_4N][Fe^{III}(2,6\text{-dimethylphenolate})_4]$ with excess RSH (R = Me, Et, *i*-Pr, Ph) gives $[R_4N][Fe(SR)_4]$ in good yield. $[Et_4N][Fe(SMe)_4]$ (**1**), $[(n\text{-}Pr)_4N][Fe(SEt)_4]$ (**2**) and $[Et_4N][Fe(SPh)_4]$ (**3**) were structurally characterized by X-ray crystallography. The $[Fe(SR)_4]^-$ anions of **1** and **2** possess crystallographic $S_4$ point group symmetry. The $[FeS_4]$ core of **2** has nearly perfect $T_d$ symmetry, whereas the $[FeS_4]$ core in **1** has a compressed $D_{2d}$ structure. The $[Fe(SPh)_4]^-$ anion has approximate $S_4$ symmetry with the $[FeS_4]$ core compressed along the $S_4$ axis. The existence of the $S_4$ and $D_{2d}$ conformation isomers in tetrahedral $[M(SPh)_4]^{n-}$ complexes is discussed. The electronic spectra, $^1H$ NMR spectra, and the electrochemistry of the $[Fe(SR)_4]^-$ complexes are reported and compared to those of $[Fe^{III}(Cys\text{-}S)_4]$ centers in proteins.

From an inorganic chemist's viewpoint, rubredoxin is the simplest of all metalloproteins; a single iron atom is coordinated by four equivalent ligands in a tetrahedral coordination geometry. Since the first report of the X-ray crystal structure of oxidized rubredoxin in 1969, there has been a recognized need for synthetic analogs for the $[Fe^{III}(Cys\text{-}S)_4]$ unit of this protein.[1a] In 1975, the synthesis of $[Fe^{III}(S_2\text{-}o\text{-xyl})_2]^-$ was reported as an analog for oxidized rubredoxin ($Rd_{ox}$).[2-4] Attempts by several groups to obtain other examples of stable $[Fe(SR)_4]^-$ complexes with monodentate thiolate ligands or with other polydentate ligands have all resulted in failure. The failure was ascribed to the apparent instability of $[Fe(SR)_4]^-$ complexes toward oligomerization reactions and/or autoredox reactions that generate Fe(II) and RSSR. The reaction of $FeCl_3$ with alkanethiolates in MeOH produces an immediate precipitate of insoluble materials of empirical formula $Fe(SR)_3$.[5] A similar reaction of $FeCl_3$ with benzenethiolate produces intensely colored transient species which rapidly undergo an autoredox reaction to produce $[Fe^{II}(SPh)_4]^{2-}$ and PhSSPh.[6] Attempts to oxidize the $[Fe^{II}(SPh)_4]^{2-}$ complex to its $[Fe^{III}(SPh)_4]^-$ redox level were also unsuccessful.[7a] In 1982, Millar discovered that stable $[Fe(SR)_4]^-$ complexes could be synthesized using monodentate thiolate ligands in the cases where the ligands were sterically hindered aromatic thiolates.[8,9] This success prompted us to reexamine the problem of the synthesis of $[Fe(SR)_4]^-$ complexes with less bulky thiolate ligands. We report herein a new and general route to the synthesis of $Fe^{III}(SR)_4]^-$ compounds.[10]

## Experimental Section

All reactions were performed with freshly distilled solvents under a nitrogen atmosphere using Schlenk techniques.

**$[Et_4N][Fe(SMe)_4]$ (1).** MeSH was bubbled through a concentrated solution of 2.06 g (3.07 mmol) of $[Et_4N][Fe(O\text{-}2,6\text{-}Me_2C_6H_3)_4]$[11] in 25 mL of DMF at 0 °C until the solution was dark red and no trace of orange color was evident. Addition of 50 mL of diethyl ether followed by cooling to −20 °C, filtration, and rinsing with ether gave 0.99 g of **1** (86% yield). This product is a dark red-black solid and is extremely air-sensitive in solution.

**$[(n\text{-}Pr)_4N][Fe(SEt)_4]$ (2).** Ethyl mercaptan (2 mL; 27.0 mmol) was added to a concentrated solution of $[(n\text{-}Pr)_4N][Fe(O\text{-}2,6\text{-}Me_2C_6H_3)_4]$ (2.91 g; 4.0 mmol) in 3–5 mL of DMF at 0 °C. The color of the solution changed immediately from orange-brown to red-black. Addition of 70 mL of ether and cooling to −20 °C precipitated black-red crystals in 90% yield (1.81 g). Anal. Calcd: C, 49.36; H, 9.94; N, 2.88; S, 26.35. Found: C, 49.58; H, 9.63; N, 2.83; S, 26.69.

**$[Et_4N][Fe(SPh)_4]$ (3).** This compound was prepared in the same manner as **2** except that 2.7 mL (3.94 mmol) of HSPh and 0.50 g (0.68 mmol) of $[Et_4N][Fe(O\text{-}2,6\text{-}Me_2C_6H_3)_4]$ produced 0.31 g (66% yield) of product. Anal. Calcd: C, 61.72; H, 6.47; N, 2.25; S, 20.59. Found: C, 61.75; H, 6.46; N, 2.42; S, 21.51.

**$[Ph_4P][Fe(S\text{-}i\text{-}Pr)_4]$.** This product was prepared in 60% yield in an analogous manner using 1.01 g (1.15 mmol) of $[Ph_4P][Fe(O\text{-}2,6\text{-}Me_2C_6H_3)_4]$ and 0.6 mL (6.46 mmol) of HS-*i*-Pr. Anal. Calcd: C, 62.14; H, 6.95; P, 4.45; S, 18.43. Found: C, 62.07; H, 6.82; P, 4.45; S, 18.30.

**$[(n\text{-}Pr)_4N][Fe(S\text{-}i\text{-}Pr)_4]$.** This product, which was prepared in 60% yield, crystallized in the tetragonal $I\bar{4}$ space group with $a = b = 10.787$ (5) and $c = 14.239$ (7) Å.

**$[Fe(S\text{-}t\text{-}Bu)_4]^-$, $[Fe(SCH_2Ph)_4]^-$, and $[Fe(SCH(Ph)CH_3)_4]^-$.** These complexes can be generated in DMF solutions using the appropriate thiols. Attempts to isolate the compounds as solids were not successful. Electronic spectra of these compounds were obtained by reacting solutions of $[Et_4N][Fe(O\text{-}2,6\text{-}Me_2C_6H_3)_4]$ in DMF with excess thiol.

**X-ray Crystallographic Structure Determination.** The general procedures for unit cell determination, data collection, and structure solution have been previously described.[12] Pertinent crystal data for the individual compounds are given in Table I.

**$[Et_4N][Fe(SMe)_4]$.** A crystal, which was obtained by cooling a DMF/diethyl ether solution of the compound, was mounted under nitrogen in a glass capillary. The tetragonal $I\bar{4}$ space group was previously observed

(1) (a) Watenpaugh, K. D.; Sieker, L. C.; Jensen, L. H. *J. Mol. Biol.* **1980**, *138*, 615–633. (b) Stenkamp, R. E.; Sieker, L. C.; Jensen, L. H. *Proteins, Struct. Funct. Genet.* **1990**, *8*, 352–364. (c) Adman, E. T.; Sieker, L. C.; Jensen, L. H. *J. Mol. Biol.* **1991**, *217*, 337–352. (d) Frey, M.; Sieker, L.; Payan, F.; Haser, R.; Bruschi, M.; Pepe, G.; LeGall, J. *J. Mol. Biol.* **1987**, *197*, 525.

(2) Lane, R. W.; Ibers, J. A.; Frankel, R. B.; Holm, R. H. *Proc. Natl. Acad. Sci. U.S.A.* **1975**, *72*, 2868–2872.

(3) Lane, R. W.; Ibers, J. A.; Frankel, R. B.; Papaefthymiou, G. C.; Holm, R. H. *J. Am. Chem. Soc.* **1977**, *99*, 84–98.

(4) Abbreviations: $S_2$-*o*-xyl = *o*-xylene-$\alpha,\alpha'$-dithiolate; S-2,3,5,6-$Me_4C_6H$ = 2,3,5,6-tetramethylbenzenethiolate; S-2,4,6-*i*-$Pr_3C_6H_2$ = 2,4,6-triisopropylbenzenethiolate; S-2-$PhC_6H_4$ = 2-phenylbenzenethiolate.

(5) Averill, B. A.; Herskovitz, T.; Holm, R. H.; Ibers, J. A. *J. Am. Chem. Soc.* **1973**, *95*, 3523–3533.

(6) Hagen, K. S.; Reynolds, J. G.; Holm, R. H. *J. Am. Chem. Soc.* **1981**, *103*, 4054.

(7) (a) Coucouvanis, D.; Swenson, D.; Baenziger, N. C.; Murphy, C.; Holah, D. G.; Sfarnas, N.; Simopoulos, A.; Kostikas, A. *J. Am. Chem. Soc.* **1981**, *103*, 3350–3362. (b) Swenson, D.; Baenziger, N. C.; Coucouvanis, D. *J. Am. Chem. Soc.* **1978**, *100*, 1932.

(8) Millar, M.; Lee, J. F.; Koch, S. A.; Fikar, R. *Inorg. Chem.* **1982**, *21*, 4105–4106.

(9) Millar, M.; Lee, J. F.; O'Sullivan, T.; Koch, S. A.; Fikar, R. Submitted for publication.

(10) Koch, S. A.; Maelia, L. E.; Millar, M. *J. Am. Chem. Soc.* **1983**, *105*, 5944–5945.

(11) Koch, S. A.; Millar, M. *J. Am. Chem. Soc.* **1982**, *104*, 5255.

(12) Lincoln, S.; Koch, S. A. *Inorg. Chem.* **1986**, *25*, 1594.

0020-1669/92/1331-4594$03.00/0 

**Table I.** Crystallographic Data for X-ray Diffraction Studies

| | $[Et_4N][Fe(SMe)_4]$ | $[(n\text{-}Pr)_4N][Fe(SEt)_4]$ | $[Et_4N][Fe(SPh)_4]$ |
|---|---|---|---|
| formula | $FeS_4NC_{12}H_{32}$ | $FeS_4NC_{20}H_{48}$ | $FeS_4NC_{32}H_{40}$ |
| fw | 374.5 | 486.7 | 622.8 |
| $a$, Å | 9.780 (3) | 10.598 (2) | 9.194 (2) |
| $b$, Å | 9.780 (3) | 10.598 (2) | 8.892 (2) |
| $c$, Å | 10.801 (2) | 12.588 (2) | 40.779 (8) |
| $\alpha$, deg | 90 | 90 | 90 |
| $\beta$, deg | 90 | 90 | 92.96 (1) |
| $\gamma$, deg | 90 | 90 | 90 |
| $V$, Å$^3$ | 1033.2 (9) | 1413.9 (8) | 3330 (2) |
| $Z$ | 2 | 2 | 4 |
| space group | $I\bar{4}$ | $I\bar{4}$ | $P2_1/n$ |
| temp | ambient | ambient | ambient |
| radiation (graphite monochromator, $\lambda$ = 0.710 73) | Mo K$\alpha$ | Mo K$\alpha$ | Mo K$\alpha$ |
| linear abs coeff, cm$^{-1}$ | 11.22 | 8.35 | 7.27 |
| scan mode | $\theta/2\theta$ | $\theta/2\theta$ | $\theta/2\theta$ |
| $2\theta$ range, deg | $0 < 2\theta < 60$ | $0 < 2\theta < 60$ | $0 < 2\theta < 44$ |
| no. of unique refins with $\lvert F_o\rvert^2 > 3\sigma\lvert F_o\rvert^2$ | 637 | 595 | 1462 |
| final no. of variables | 41 | 95 | 314 |
| $R^a = \sum[\lvert F_o\rvert - \lvert F_c\rvert]/\sum\lvert F_o\rvert$ | 0.0314 | 0.050 | 0.0584 |
| $R_w = [\sum w(\lvert F_o\rvert - \lvert F_c\rvert)^2/\sum wF_o^2]^{1/2}$ | 0.0314 | 0.067 | 0.0750 |
| std error in observn of unit wt | 0.744 | 2.08 | 2.103 |

[a] Quantity minimized: $(\sum w(\lvert F_o\rvert - \lvert F_c\rvert)^2)$; weight $w = 1/(\sigma^2 + 0.0016F_o^2)$.

for other $[M(SR)_4]^-$ complexes.[8,9,13] The structure solution is completely analogous to that described for $[(n\text{-}Pr)_4N][Ga(SEt)_4]$.[13] The hydrogen positions were calculated for the cation and located in a difference Fourier map for the anion. The hydrogen atoms were used in the structure factor calculations but were not refined. Least-squares refinement with all non-hydrogen atoms anisotropic gave $R$ ($R_w$) = 0.0434 (0.0442). Refinement of the coordinates for the opposite enantiomer resulted in a substantial drop in the $R$ values with $R$ ($R_w$) = 0.0314 (0.0314). The final atomic coordinates are given in the supplementary material.

**$[(n\text{-}Pr)_4N][Fe(SEt)_4]$.** This complex also crystallizes in the tetragonal space group $I\bar{4}$ and is isomorphous with $[(n\text{-}Pr)_4N][Ga(SEt)_4]$.[13] The ethyl carbons of the thiolate ligands and methylene carbons of the cation were disordered. The multiplicities of these carbons were refined and then fixed at 0.6 and 0.4 for C$n$ and C$n$A, respectively ($n$ = 1–4). No hydrogen positions were calculated due to the disorder in both the cation and anion. After each enantiomer was tested, final $R$ ($R_w$) = 0.0502 (0.0671). The atomic coordinates are given in the supplementary material.

**$[Et_4N][Fe(SPh)_4]$.** The monoclinic space group $P2_1/c$ with $Z$ = 4 indicates that there is no crystallographic symmetry imposed on this compound. Direct methods were used to provide the coordinates of the iron and the four sulfur atoms. The methylene carbons in the cations were disordered with multiplicities of 0.8 and 0.2 for C$n$1 and C$n$1B ($n$ = 5–8). Final least-squares refinement gave $R$ ($R_w$) = 0.0584 (0.0756). The final atomic coordinates are given in the supplementary material.

## Results and Discussion

**Synthesis of $[Fe^{III}(SR)_4]^-$ Complexes.** A new route to the synthesis of $[Fe^{III}(SR)_4]^-$ complexes has been developed that involves an acid–base ligand-exchange reaction of thiol with coordinated phenolate:

$$[Fe^{III}(OPh)_4]^- + 4RSH \rightarrow [Fe^{III}(SR)_4]^- + 4PhOH$$

The ligand-exchange reaction appears to be a completely general one. Solutions containing stable $[Fe(SR)_4]^-$ complexes can be easily produced by the addition of the appropriate thiol to DMF solutions of $[Fe(O\text{-}2,6\text{-}Me_2C_6H_3)_4]^-$.[11] The reactions can be monitored by absorption spectroscopy; the two low-energy bands in the spectrum of the phenolate complex are shifted to lower energy as the phenolate ligands are replaced by the thiolates (Figure 1). Although solutions of $[Fe(SR)_4]^-$ complexes are readily formed in situ, isolation of pure materials from these solutions proved to be difficult due to the extreme sensitivity of the complexes. For example, addition of alcohol to the DMF solution of $[Fe(SR)_4]^-$, where R = alkyl, produces substantial amount of a green insoluble material that is likely $[Fe(SR)_3]_x$.[5] Under other conditions, the intense red solutions of the $[Fe(SR)_4]^-$ were observed to bleach, a behavior which is indicative of the occurrence of the autoredox reaction $Fe^{III}(SR) \rightarrow Fe(II) + {}^1/_2RSSR$. We found that in many cases it was advantageous to first prepare the corresponding $[Ga^{III}(SR)_4]^-$ complex and then to apply the information gained concerning cations of crystallization, solvents, and methods of crystallization to the synthesis of an assumed isomorphous iron complex.[13] Gallium thiolates do not undergo the autoredox reactions. Also, in almost all the cases investigated, the Ga(III) and the Fe(III) complexes proved to be isomorphous.

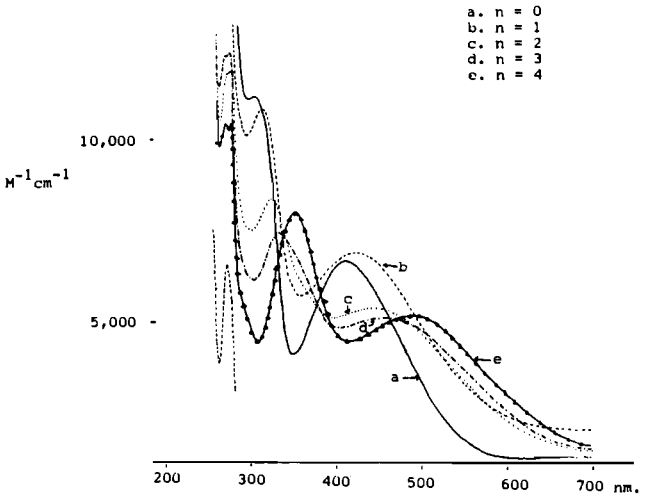


**Figure 1.** Thiol-ligand-exchange reaction of $[Fe(O\text{-}2,6\text{-}Me_2C_6H_3)_4]^-$ with EtSH as monitored by absorption spectroscopy.

The starting material for the reactions, $[R_4N][Fe(O\text{-}2,6\text{-}Me_2C_6H_3)_4]$, is readily made in one step, in high yield, from inexpensive starting materials: $FeCl_3$, $[Li(O\text{-}2,6\text{-}Me_2C_6H_3)]$, and $R_4NBr$.[11] Our rationale for the success of the ligand-exchange reaction involves several points. The phenolate ligands stabilize the Fe(III) oxidation level of the starting material and intermediates during the synthesis; the reduction potential of $[Fe(O\text{-}2,6\text{-}Me_2C_6H_3)_4]^-$ is very negative (–1.30 V vs SCE) as compared with the potential of $[FeCl_4]^-$, which is –0.08 V.[14] The acidity of thiols is generally greater than that of phenols. The relative strength of the Fe–S versus the Fe–O bonds is another driving force for the exchange reaction. Although the reactions seem to occur with stoichiometric amounts of thiols, the use of excess thiol ensures complete substitution and does not affect the

(13) Maelia, L. E.; Koch, S. A. *Inorg. Chem.* **1986**, *25*, 1896–1904.

(14) Rollick, K. L.; Kochi, J. K. *Organometallics* **1982**, *1*, 725–732.

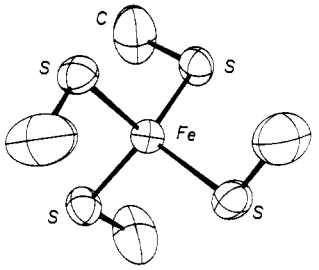


**Figure 2.** ORTEP diagram of the anion of $[Et_4N][Fe(SMe)_4]$ (view down the crystallographic $S_4$ axis).

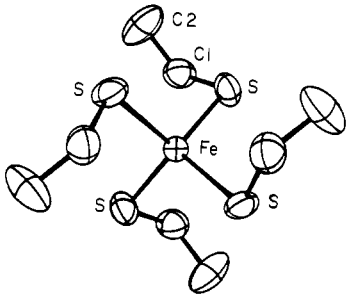


**Figure 3.** ORTEP diagram of the anion of $[(n\text{-}Pr)_4N][Fe(SEt)_4]$ (view down the crystallographic $S_4$ axis).

stability of the product. A key feature of our work was the discovery of the solvent conditions under which the $[Fe(SR)_4]^-$ complexes are stable; the ligand-exchange reactions are successful in polar aprotic solvents such as DMF, DMSO, and $CH_3CN$. It is likely that some of the previous attempts to obtain these compounds failed because the $[Fe(SR)_4]^-$ complexes were generated in solvents (e.g. alcohols) in which they are unstable. $[Fe(SPh)_4]^-$ has recently been generated in solution by ligand substitution of $[Fe(S_2\text{-}o\text{-}xyl)_2]^-$ with PhSSPh[15] and by $[Fe(CN)_6]^{3-}$ oxidation of $[Fe(SPh)_4]^{2-}$.[16]

The ligand-exchange reaction was also applied to the synthesis of $[Fe(S_2\text{-}o\text{-}xyl)_2]^-$, $[Fe(S\text{-}2,3,5,6\text{-}Me_4C_6H)_4]^-$, and $[Fe(S\text{-}2,4,6\text{-}i\text{-}Pr_3C_6H_2)_4]^-$, which were the only previously known examples of stable $[Fe^{III}(SR)_4]^-$ complexes.[2,3,9,30] All three of these complexes were previously prepared by air oxidation of the corresponding $[Fe(SR)_4]^{2-}$ complex, which was generated from the reaction of $Fe^{II}Cl_2$ with excess thiolate. The last two complexes were also prepared by the direct reaction of $FeCl_3$ with excess thiolate. Another advantage of the thiol-exchange reaction over the previous synthetic routes is that near-quantitative yields can be obtained. This is particularly valuable for syntheses in which isotopically enriched iron or costly thiolate ligands are used.

**Structures of $[Fe(SMe)_4]^-$ and $[Fe(SEt)_4]^-$.** Both $[Et_4N][Fe(SMe)_4]$ (**1**) and $[(n\text{-}Pr)_4N][Fe(SEt)_4]$ (**2**) crystallize in the tetragonal space group $I\bar{4}$ with $Z = 2$. The crystal symmetry requires that both the cations and the anions possess rigorous $S_4$ point group symmetry. Both complexes are also isomorphous with their Ga(III) analogs.[13] ORTEP diagrams of the anions of **1** and **2** viewed down the crystallographic $S_4$ axis are shown in Figures 2 and 3. The $[FeS_4]$ cores are required to have exact $D_{2d}$ symmetry. The $[FeS_4]$ core in **1** is distorted from $T_d$ symmetry by a compression along the $S_4$ axis (Table II). This compression produces two S–Fe–S angles (labeled a in Figure 4) greater than the tetrahedral; angle of 109.5°, at 114.24 (8)°, and four compressed angles (labeled b) less than 109.5°, at 107.14 (4)°. The $[FeS_4]$ core in **2** has nearly perfect $T_d$ symmetry with S–Fe–S angles of 109.69 (9) and 109.36 (5)° (Table III). The $S_4$ symmetry of the anions allows for only a single Fe–S bond length that is 2.264 (1) Å in **1** and 2.269 (1) Å in **2**. The tetragonal

**Table II.** Selected Bond Distances (Å) and Angles (deg) for $[Et_4N][Fe(SMe)_4]$

| | | | |
|---|---|---|---|
| Fe–S | 2.264 (1) | S–Fe–S′ [a] | 114.24 (8) ×2 |
| S–C1 | 1.753 (8) | S–Fe–S″ [a] | 107.14 (4) ×4 |
| | | Fe–S–C1 | 103.9 (3) |
| N–C2 | 1.516 (5) | C2–N–C2 | 111.2 (4) ×2 |
| C2–C3 | 1.500 (7) | C2–N–C2 | 108.6 (2) ×4 |
| S′–Fe–S–C1 [a,b] | −54.5 | N–C2–C3 | 115.6 (4) |

[a] S′ is related to S by a $C_2$ ($S_2^4$) rotation about the $S_4$ axis; S″ is related to S by an $S_4$ rotation. [b] Torsion angle.

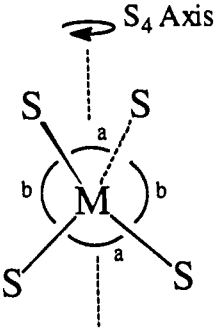


**Figure 4.** Diagram showing the distortion of a $[MS_4]$ unit along an $S_4$ axis.

**Table III.** Selected Bond Distances (Å) and Angles (deg) for $[(n\text{-}Pr)_4N][Fe(SEt)_4]$

| | | | |
|---|---|---|---|
| Fe–S | 2.269 (1) | S–Fe–S′ [a] | 109.69 (9) ×2 |
| S–C1 | 1.80 (2) | S–Fe–S″ [a] | 109.36 (5) ×4 |
| S–C1A | 1.96 (5) | Fe–S–C1 | 104.9 (5) |
| S′–Fe–S–C1 [a,b] | 57.0 | Fe–S–C1A | 99.3 (7) |
| S′–Fe–S–C1A [a,b] | 72.4 | | |

[a] S′ is related to S by a $C_2$ ($S_2^4$) rotation about the $S_4$ axis; S″ is related to S by an $S_4$ rotation. [b] Torsion angle.

compression of the $[FeS_4]$ core of **1** is nearly identical to that observed in $[Et_4N][Fe^{III}(S\text{-}2,3,5,6\text{-}Me_4C_6H)_4]$ (**4**), which also crystallizes in the $I\bar{4}$ space group.[8,9]

The $[Fe(S\text{-}\alpha\text{-}C)_4]$ units in **1**, **2**, and **4** have $S_4$ symmetry. The location of the $\alpha$-carbon is responsible for defining the orientation of the three sulfur p orbitals which are responsible for the $\sigma$ and $\pi$ bonding between S and the metal.[8-10] The dihedral angle between the S–Fe–S plane and the Fe–S–C plane is 87.4° in $[Et_4N][Fe(S\text{-}2,3,5,6\text{-}Me_4C_6H)_4]$ and 54.5° in **1**. The Fe–S–C angles in **1**, **2**, and **4** are in the range 99–105°.

The unit cell determinations of $[(n\text{-}Pr)_4N][Fe(S\text{-}i\text{-}Pr)_4]$ and its Ga(III) analog show that these compounds also crystallize in the tetragonal space group $I\bar{4}$ with $Z = 2$. The tetragonal crystal symmetry found for **1**, **2**, $[(n\text{-}Pr)_4N][Fe(S\text{-}i\text{-}Pr)_4]$, and $[Et_4N][Fe(S\text{-}2,3,5,6\text{-}Me_4C_6H)_4]$[8,9] and their gallium analogs[13] makes these complexes ideal candidates for single-crystal spectroscopic studies.[17]

**Structure of $[Fe^{III}(SPh)_4]^-$ and Related $[M(SPh)_4]^{n-}$ Compounds.** Although the $[Fe^{III}(SPh)_4]^-$ anion in **3** does not possess any crystallographic symmetry, the ORTEP view in Figure 5 shows that the geometry of the entire anion has idealized $S_4$ point group symmetry. The four Fe–S bond lengths range from 2.289 (3) to 2.307 (3) Å, with an average value of 2.297 (6) Å (Table IV). The $[FeS_4]$ core is a distorted tetrahedron compressed along the pseudo-$S_4$ axis with the two angles bisected by this axis equal to 114.4 (1) and 115.2 (1)° and the four remaining angles equal to 105.9 (1), 107.1 (1), 110.8 (1), and 103.7 (1)°. The Fe–SPh groups are approximately planar. The dihedral angle between the plane of a phenyl ring and the corresponding Fe–S–C plane ranges from 9.4 to 27.1°.

(15) Yanada, K.; Nagano, T.; Hirobe, M. *Chem. Pharm. Bull.* **1983**, *31*, 4589–4592.
(16) Mascharak, P. K. *Inorg. Chem.* **1986**, *25*, 245–247.
(17) (a) Deaton, J. C.; Gebhard, M. S.; Koch, S. A.; Millar, M.; Solomon, E. I. *J. Am. Chem. Soc.* **1988**, *110*, 6241. (b) Gebhard, M. S.; Deaton, J. C.; Koch, S. A.; Millar, M.; Solomon, E. I. *J. Am. Chem. Soc.* **1990**, *112*, 2217.,

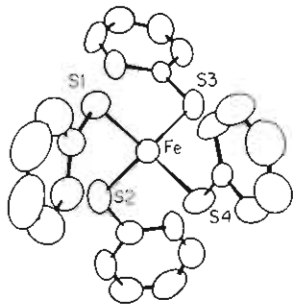


**Figure 5.** ORTEP diagram of the anion of $[Et_4N][Fe(SPh)_4]$ (view down the approximate $S_4$ axis in the anion).

**Table IV.** Selected Bond Distances (Å) and Angles (deg) for $[Et_4N][Fe(SPh)_4]$

| | | | |
|---|---|---|---|
| Fe–S1 | 2.296 (3) | Fe–S4–C41 | 108.3 (5) |
| Fe–S2 | 2.296 (3) | S1–Fe–S2 | 105.9 (1) |
| Fe–S3 | 2.289 (3) | S1–Fe–S3 | 107.1 (1) |
| Fe–S4 | 2.307 (3) | S1–Fe–S4 | 114.4 (1) |
| Fe–S1–C11 | 113.1 (4) | S2–Fe–S3 | 115.2 (1) |
| Fe–S2–C21 | 112.4 (4) | S2–Fe–S4 | 110.8 (1) |
| Fe–S3–C31 | 112.3 (4) | S3–Fe–S4 | 103.7 (1) |

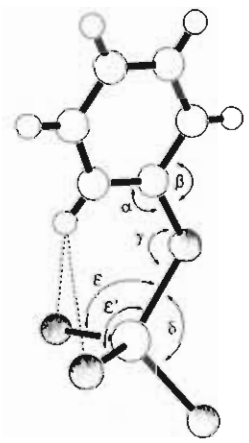


**Figure 6.** Diagram showing the conformation of an SPh ligand with respect to the $FeS_4$ core and some of the parameters that define this interaction.


I II

**Figure 7.** Diagrams showing two conformations involving the orientation of the aromatic ring with respect to the M–S–C plane.

The plane of each phenyl ring is perpendicular to, and approximately bisects, a triangular $S_3$ face of the $S_4$ tetrahedron (see Figure 6). These dihedral angles range from 87.3 to 113.5°.[18]

This fundamental in-plane configuration (I in Figure 7) of the M–SPh was recognized by Coucouvanis in the structure of $[PPh_4]_2[Fe^{II}(SPh)_4]$ and is quite common for terminal benzenethiolate ligands bound to tetrahedral $[S_3MSPh]$ centers.[7] Much less common is the conformation in which the plane of the phenyl ring is orthogonal to its M–S–C plane (II in Figure 7). The in-plane conformation is more stable than the out-of-plane conformation since, in the former case, the $3p\pi$ nonbonding orbital of the sulfur is conjugated with the phenyl ring. An analogous conformational preference has been observed for aromatic thiols, aromatic sulfides, phenols, and phenolate ethers.[19] The presence

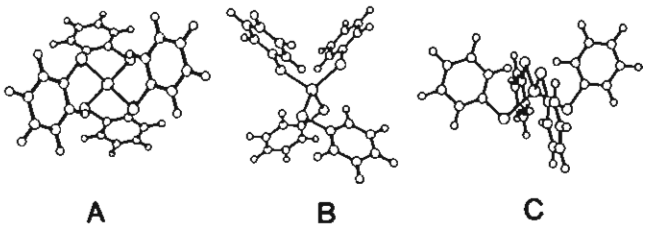


**Figure 8.** Diagrams of idealized $S_4$ and $D_{2d}$ structures of tetrahedral $[M(SPh)_4]$ compounds: (A and B) different views of the $S_4$ conformation isomer; (C) $D_{2d}$ isomer.

of ortho substituents on the phenyl ring results in the out-of-plane M–S–Ar conformation (e.g., $[Fe(S\text{-}2,3,5,6\text{-}Me_4C_6H)_4]^-$).[8,9]

The close approach of one of the phenyl ortho hydrogens to the sulfurs on the tetrahedral face that the phenyl ring intercepts causes a repulsion between the phenyl hydrogens and the sulfurs. Figure 6 defines the parameters used by Coucouvanis to describe these interactions.[7] Referring to the parameters in Figure 6, the $\alpha$ and $\gamma$ angles are enlarged and the $\beta$ angle is compressed as the phenyl ring is pushed away. The angles $\epsilon$ and $\epsilon'$ become larger than 109.5°, and the angle $\delta$ becomes less than 109.5°. Using this simple structural analysis, Coucouvanis was able to show that the distortions observed in the $[MS_4]$ core of $[PPh_4]_2[Fe^{II}(SPh)_4]$ and its isostructural Mn(II), Co(II), Ni(II), Zn(II), and Cd(II) complexes are the result of the combined interaction of the four thiolate ligands with the $[MS_4]$ core.[7]

We have been able to add an important stereochemical aspect to the analysis of the structure of tetrahedral $[M(SPh)_4]$ compounds.[10] If one assumes the basic-in-plane conformation of the individual M–S–Ph groups and the phenyl ortho hydrogen–$[MS_4]$ interaction, the overall geometry of the $[M(SPh)_4]$ unit can have only two possible types of conformations, both of which have high idealized symmetry: the $D_{2d}$ geometry observed in $[PPh_4]_2[Fe^{II}(SPh)_4]$[7] and the $S_4$ geometry observed in $[Et_4N][Fe^{III}(SPh)_4]$. Figure 8 shows diagrams of the $S_4$ and $D_{2d}$ isomers that were drawn from coordinates with the exact symmetries. Visual comparison of the structures determined by X-ray diffractometry and the precise structures reveals the basic structural congruence.

An application of Coucouvanis's structural analysis to the $S_4$ isomer, in general and to $[Et_4N][Fe^{III}(SPh)_4]$, in particular, reveals that the $[MS_4]$ core is compressed along the $S_4$ axes.[20] This is in contrast to the predicted and observed elongations along the $S_4$ axis in the $D_{2d}$ case. The change in the sign of the tetragonal distortions of the $[MS_4]$ core in the $S_4$ and $D_{2d}$ isomers results from the different distributions of the angles defined as $\epsilon$ and $\delta$ among the S–M–S angles of the $MS_4$ cores. This analysis predicts that the deviations from 109.5° should be larger for the S–M–S angles in the $D_{2d}$ isomer.

The energy difference between the $D_{2d}$ and the $S_4$ conformational isomers is small; in several cases, both the $S_4$ and the $D_{2d}$ isomers have been structurally characterized for the same metal ion (Table V). $[Ph_4P]_2[Fe(SPh)_4]$ has the $D_{2d}$ structure, while $[Et_4N]_2[Fe(SPh)_4]$[7] and $[Et_4N]_2[Fe(p\text{-}SC_6H_4CH_3)_4]$ have the $S_4$ structure.[21] $[Ph_4P]_2[Ni(SPh)_4]$ and $[Et_4N]_2[Ni(S\text{-}p\text{-}C_6H_4Cl)_4]$ have $D_{2d}$ structures, while $[Et_4N]_2[Ni(SPh)_4]$ has the $S_4$ structure.[7,22,23] In neither the Fe(II) nor the Ni(II) case was the symmetry of the $S_4$ isomers previously recognized; the published ORTEP diagrams are not ones in which the overall $S_4$ symmetry of the anions is obvious.[51] The $S_4$ axis in $[Et_4N]_2[Ni(SPh)_4]$

(18) A table of least-squares planes and dihedral angles is given in the supplementary material.
(19) Romm, I. P.; Gur'yanova, E. N. *Russ. Chem. Rev. (Engl. Transl.)* **1986**, *55*, 83–98.
(20) A table of parameters for $[Et_4N][Fe(SPh)_4]$ is given in the supplementary material.
(21) Beisheng, K.; Jinua, C. *Jiegou Huaxue* **1985**, *4*, 119. This structure is included in the Cambridge Structural Database.
(22) Yamamura, T.; Miyamae, H.; Katayama, Y.; Sasaki, Y. *Chem. Lett.* **1985**, 269–272.
(23) Rosenfield, S. G.; Armstrong, W. H.; Mascharak, P. K. *Inorg. Chem.* **1986**, *25*, 3014–3018.

**Table V.** Structures of $[M(SAr)_4]^{n-}$ Compounds

| compound | symmetry of $[M(SPh)_4]^{n-}$ | M–S, Å | S–M–S angles bisected by $S_4$ axis, deg | S–M–S, deg |
|---|---|---|---|---|
| $[Ph_4P]_2[Fe^{II}(SPh)_4]$[7] | $D_{2d}$ | 2.353 | 97.8, 101.3 | 119.0, 112.7, 111.5, 115.3 |
| $[Et_4N]_2[Fe^{II}(S\text{-}p\text{-tolyl})_4]$[21] | $S_4$ | 2.34 | 116.8, 117.2 | 111.6, 109.5, 101.4, 101.2 |
| $[Et_4N][Fe^{III}(SPh)_4]$ | $S_4$ | 2.297 | 114.4, 115.2 | 105.9, 107.1, 110.8, 103.7 |
| $[Ph_4P]_2[Zn(SPh)_4]$[7] | $D_{2d}$ | 2.353 | 96.7, 99.6 | 121.0, 115.6, 112.6, 112.5 |
| $[Me_4N]_2[Zn(SPh)_4]$[28] | $S_4$ | 2.357 | 117.2, 113.7 | 103.9, 112.1, 110.4, 99.9 |
| $[Me_4N]_2[Hg(S\text{-}p\text{-}C_6H_4Cl)_4]$[50] | $D_{2d}$ | 2.545 | 101.75, 101.75 | 109.8, 119.4, 109.8, 119.4 |
| $[Ph_4P]_2[Ni^{II}(SPh)_4]$[7] | $D_{2d}$ | 2.288 | 92.0, 92.7 | 124.9, 117.9, 116.3, 115.4 |
| $[Et_4N]_2[Ni^{II}(SPh)_4]$[a,22] | $S_4$ | 2.292 | 118.6, 123.7 | 109.1, 97.2, 105.2, 104.4 |
| $[Et_4N]_2[Ni^{II}(S\text{-}p\text{-}C_6H_4Cl)_4]$[23] | $D_{2d}$ | 2.281 | 88.1, 89.9 | 122.4, 121.9, 114.1, 123.8 |
| $[Me_4N]_2[Cd(SPh)_4]$[28] | $S_4$ | 2.541 | 116.6, 112.1 | 105.1, 113.8, 110.5, 98.9 |
| $[NEt_4]_2[Fe^{II}(SePh)_4]$[b,29] | $S_4$ | 2.460 | 114.9, 114.6 | 105.6, 111.7, 103.6, 106.3 |
| $[Et_4N]_2[Fe^{II}(S\text{-}2\text{-}PhC_6H_4)_4]$[27] | $S_4$ | 2.338 | 113.4, 113.4 | 107.5, 107.5, 107.5, 107.5 |

[a] $S_4$ axis bisects the angles S1–Ni–S2 and S3–Ni–S4. [b] $S_4$ axis bisects the angles Se1–Fe–Se3 and Se2–Fe–Se4.

bisects the angles, S1–Ni–S2 and S3–Ni–S4.[22] In the $S_4$ isomers of the Fe(II) and Ni(II) anions, the $[MS_4]$ cores are compressed from $T_d$ along the pseudo-$S_4$ axes, as was the case for $[Et_4N][Fe^{III}(SPh)_4]$ (Table V). The existence of both tetragonally compressed and elongated $[NiS_4]$ tetrahedral cores in $[Ni(SPh)_4]^{2-}$ complexes is interesting, since the factors that determine the geometry of $[Ni^{II}(SR)_4]$ complexes are not well understood.[23-27] The conformational effects exhibited in the $[M(SPh)_4]^{n-}$ anions also appear to govern the structures of Se analogs. $[Me_4N]_2[Zn(SePh)_4]$, $[Me_4N]_2[Cd(SePh)_4]$, and $[Et_4N]_2[Fe^{II}(SePh)_4]$ have the $S_4$ conformation.[28,29] Again, the published ORTEP diagram of $[Et_4N]_2[Fe^{II}(SePh)_4]$ concealed the $S_4$ symmetry of its $[M(SePh)_4]^{2-}$ anion.[29]

With one exception, all $[M(SPh)_4]^{n-}$ complexes reported to date are in agreement with the structural analysis; i.e., they have either the $D_{2d}$ or the $S_4$ conformation of the $[M(SPh)_4]$ anion (Table V). $[Et_4N][Ga(SPh)_4]$ is the exception: two of the Ga–SPh groups have the in-plane conformation, while the other two Ga–SPh groups have the out-of-plane conformation.[13] There is also very good agreement with the prediction of compressed $[MS_4]$ cores for the $S_4$ isomers and elongated $[MS_4]$ cores for the $D_{2d}$ isomers (Table V). In the idealized case, the $[MS_4]$ cores for both $[M(SPh)_4]^{n-}$ conformations should have exact $D_{2d}$ symmetry. In the reported compounds, there are significant distortions from rigorous $D_{2d}$ symmetry. These distortions are likely the result of intramolecular effects (e.g., the M–SPh groups are not perfectly coplanar) and/or crystal packing between the ions. Tetrahedral $ML_4$ complexes of the first-row transition metals are easily distorted. We have recently characterized an isostructural series of compounds $[Et_4N]_2[M^{II}(S\text{-}2\text{-}Ph\text{-}C_6H_4)_4]$ (M = Mn, Fe, Co, Ni, Zn, Cd, Hg) in which the entire $[M(SAr)_4]^{2-}$ anions have crystallographic $S_4$ symmetry; these compounds have $[MS_4]$ cores which have rigorous $D_{2d}$ symmetry.[27,30] In agreement with the structural analysis, their $[MS_4]$ cores are compressed along the $S_4$ axis. It can be concluded that the distortion of the $[MS_4]$ core in $[M(SPh)_4]$ complexes results primarily from the intramolecular interactions between the thiolate ligands and the $[MS_4]$ core; crystal packing forces have a secondary effect on the distortions.

The thiolate-induced distortions of the $[FeS_4]$ core of the $[Fe(SPh)_4]^{n}$ (n = 1–, 2–) complexes have a valuable relevance to the structure of the metal center in rubredoxin. It has been noted that the Mössbauer spectra of reduced rubredoxin are in closer agreement with the spectra of $[Ph_4P]_2[Fe(SPh)_4]$ rather than with those of $[Fe(S_2\text{-}o\text{-}xyl)_2]^{2-}$.[7] This is in spite of the fact that $[Ph_4P]_2[Fe(SPh)_4]$ does not possess the more biologically appropriate alkanethiolate ligands. The $D_{2d}$ arrangement of the $[Fe(S\text{-}\alpha\text{-}C)_4]$ unit and the elongated tetragonally distorted $[FeS_4]$ core in $[Ph_4P]_2[Fe(SPh)_4]$ are nearly identical with those found in rubredoxin.[7-9]

There is an interesting trend in the observed Fe–S bond lengths in the various $[Fe(SR)_4]^-$ compounds. The Fe–S distance in $[Fe(SPh)_4]^-$ (2.297 (6) Å) is significantly longer than the distances in the alkanethiolate complexes, $[Fe(SMe)_4]^-$ (2.264 (1) Å), $[Fe(SEt)_4]^-$ (2.269 (1) Å), and $[Fe(S_2\text{-}o\text{-}xyl)_2]^-$ (2.267 (3) Å). It is also longer than the distances in $[Fe(S\text{-}2,3,5,6\text{-}Me_4C_6H)_4]^-$ (2.283 (2) Å) and in $[Fe(S\text{-}2,4,6\text{-}i\text{-}Pr_3C_6H_2)_4]^-$ (2.27 (2) Å), which possess bulky substituents in the ortho positions.[8,9,31] The differences in the Fe–S distances can be related to the electron-donating capacity of the thiolate ligand. Alkanethiolates are better than aromatic thiolates. The sterically hindered thiolate ligands are better donors than benzenethiolate due to the presence of the electron-donating alkyl substituents. Alternate explanations for the longer Fe–S distances in $[Fe(SPh)_4]^-$ must also be considered. It has been suggested that the length of the individual Fe–S bonds in $Rd_{ox}$ is inversely related to the magnitude of the associated Fe–S–C angles.[32] The metrical parameters observed for the $[Fe^{III}(SR)_4]^-$ compounds do not appear to provide support for this proposal. The increase in the Fe–S–C angles in $[Fe(SPh)_4]^-$ (112 (2)°) (compared to those in $[Fe(S\text{-alkyl})_4]^-$ complexes) results from the in-plane conformation of the Fe–SPh moiety. The Fe–S–C angles in $[Fe(SPh)_4]^-$ are also 10° larger than the similar angles in $[Fe(S\text{-}2,3,5,6\text{-}Me_4C_6H)_4]^-$ (102.7 (2)°), which has the out-of-plane conformation of the aromatic thiolate ligands. It has also been suggested that the difference in the Co–S distances in $[Co(edt)_2]^{2-}$ (2.284 (6) Å) and $[Co(SPh)_4]^{2-}$ (2.328 (11) Å) is of presumed steric origin.[33] Contradicting this explanation is the observation that the Ga–S distances in $[Ga(SPh)_4]^-$ (2.26 (1) Å) are not longer than those in $[Ga(SEt)_4]^-$ (2.264 (3) Å).[13] We have previously discussed factors which affect Fe(III)–S bond distances in $[FeS_4]$ centers.[13]

The Fe–S distances in oxidized rubredoxins have been determined by X-ray crystallography for *Clostridium pasteurianium* (2.29 (3) Å),[1a] *Desulfovibrio desulfuricans* (2.275 Å),[1b] *Desulfovibrio vulgaris* (2.29 Å),[1c] and *Desulfovibrio gigas* (2.29 Å)[1d] and by EXAFS for *C. pasteurianium* (2.267 (3) Å)[34] and *Pseudomonas aerogenes* (2.265 (13) Å).[35] The Fe–S distances in the alkanethiolate complexes are in good agreement with the values from the EXAFS measurements.

(24) Davison, A.; Switkes, E. S. *Inorg. Chem.* **1971**, *10*, 837.
(25) Davison, A.; Reger, D. L. *Inorg. Chem.* **1971**, *10*, 1967.
(26) Klāui, W.; Schmidt, K.; Bockmann, A.; Brauer, D. J.; Wilke, J.; Lueken, H.; Elsenhans, U. *Inorg. Chem.* **1986**, *25*, 4125–4130.
(27) Silver, A.; Koch, S. A.; Millar, M. Submitted for publication.
(28) Ueyama, N.; Sugawara, T.; Sasaki, K.; Nakamura, A.; Yamashita, S.; Wakatsuki, Y.; Yamazaki, H.; Yasuoka, N. *Inorg. Chem.* **1988**, *27*, 741.
(29) McConnachie, J. M.; Ibers, J. A. *Inorg. Chem.* **1991**, *30*, 1770.
(30) Gebhard, M. S.; Koch, S. A.; Millar, M.; Devlin, F. J.; Stephens, P. J.; Solomon, E. I. *J. Am. Chem. Soc.* **1991**, *113*, 1640.
(31) Millar, M.; Koch, S. A.; Fikar, R. *Inorg. Chim. Acta* **1984**, *88*, L15–L16.
(32) Ueyama, N.; Sugawara, T.; Tatsumi, K.; Nakamura, A. *Inorg. Chem.* **1987**, *26*, 1978.
(33) Rao, Ch. Pulla, Dorfman, J. R.; Holm, R. H. *Inorg. Chem.* **1986**, *25*, 428.
(34) Bunker, B.; Stern, E. A. *Biophys. J.* **1977**, *19*, 253–264.
(35) Schulman, R. G.; Eisenberger, P.; Teo, B. K.; Kincaid, B. M.; Brown, G. S. *J. Mol. Biol.* **1978**, *124*, 305–321.

**Table VI.** Electronic Spectral Data for Oxidized Rubredoxin and Its Synthetic Analogs

| compound | solvent | wavelength, nm ($M^{-1}$ $cm^{-1}$) | | | |
|---|---|---|---|---|---|
| $[Et_4N][Fe(SMe)_4]$ | DMF | 277 sh (6200) | 353 (11 200) | 498 (6500) | |
| $[(n\text{-}Pr)_4N][Fe(SEt)_4]$ | DMF | 284 (4400) | 356 (10 000) | 496 (5900) | |
| $[Ph_4P][Fe(S\text{-}i\text{-}Pr)_4]$ | DMF | 290 (4200) | 357 (9200) | 500 (5500) | |
| $[Et_4N][Fe(S\text{-}t\text{-}Bu)_4]$[a] | DMF | 306 (4500) | 358 (9000) | 505 (4800) | |
| $[Et_4N][Fe(SCH_2Ph)_4]$[a] | DMF | | 357 (11 000) | 498 (6000) | |
| $[Et_4N][Fe(SCH(Ph)CH_3)_4]$[a] | DMF | | 362 (11 500) | 500 (6400) | |
| $[Ph_4P][Fe(SPh)_4]$ | DMF | | 342 (12 400) | 556 (10 000) | |
| | | | 387 sh (12 400) | | |
| $[Et_4N][Fe(S\text{-}2,3,5,6\text{-}Me_4C_6H)_4]$[8,9] | $CH_3CN$ | 295 (14 300) | 344 (6880) | 450 (7230) | |
| $[Ph_4P][Fe(S\text{-}2,4,6\text{-}i\text{-}Pr_3C_6H_2)_4]$[9] | $CH_3CN$ | 288 (11 300) | 347 (8870) | 470 (12 500) | |
| $[Et_4N][Fe(S_2\text{-}o\text{-}xyl)_2]$[2,3] | DMF | | 354 (7850) | 487 (5400) | 640 (1600) |
| | | | | | 688 (1670) |
| $FeCl_3{\cdot}6H_2O$ + Z-Cys-Thr-Val-Cys-OMe[46] | DMSO | | 350 (4700) | 495 (3100) | |
| $Rd_{ox}$ (*Clostridium pasteurianum*)[37] | $H_2O$ | | 380 (10 900) | 490 (8900) | 565 (~4000) |

[a] Generated in solution.

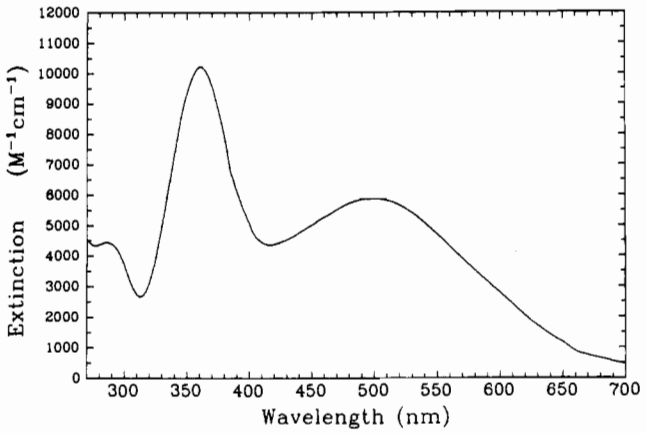


**Figure 9.** Electronic spectrum of $[(n\text{-}Pr)_4N][Fe(SEt)_4]$ in DMF.

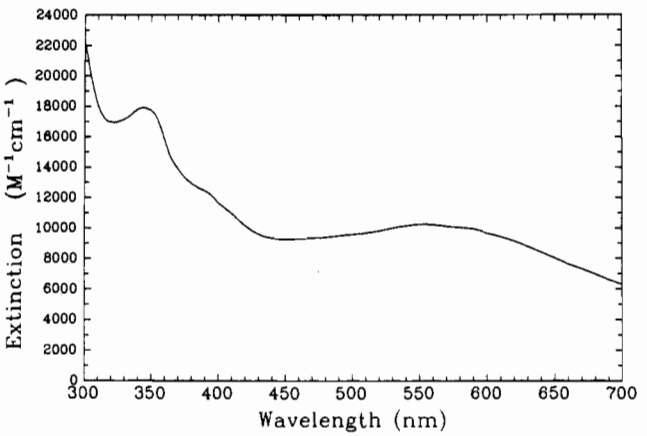


**Figure 10.** Electronic spectrum of $[Et_4N][Fe(SPh)_4]$ in DMF.

**Electronic Spectroscopy.** The electronic spectra of the $[Fe^{III}(SR)_4]$ centers in proteins and in the model compounds show distinctive differences that are related to the structures of the $[FeS_4]$ core and the $[Fe(S\text{-}\alpha\text{-}C)_4]$ units.[8,9,17,30] Except for that of the $[Fe^{III}(SPh)_4]^-$ compound, the solution electronic spectra of $[Fe(SR)_4]^-$ complexes for all monodentate thiolates are quite similar (Table VI). Each possess two broad intense bands in the regions of 350 and 500 nm (Figure 9). Oxidized rubredoxins also possess similar transitions; however, in rubredoxin each of these transitions displays further splitting.[36,37] The electronic spectrum of $[Fe(S_2\text{-}o\text{-}xyl)_2]^-$ shows significant splitting of the low-energy band; the splitting is different from that observed for rubredoxins.[2,3]

The solution spectrum of $[Fe(SPh)_4]^-$ differs substantially from that of the other monodentate alkanethiolate $[Fe(SR)_4]^-$ complexes. In the spectrum of $[Fe(SPh)_4]^-$, there are two bands at 342 and 387 nm and a very broad band at 556 nm, which tails toward the near-IR region (Figure 10). The distortions in the $[FeS_4]$ core, which are present in the solid-state structure of $[Fe(SPh)_4]^-$, should also be found in solution. It is also likely that both the $S_4$ and the $D_{2d}$ conformation isomers are present in solution. In the absence of the special geometric constraints found for the $[Fe(SPh)_4]^-$ complex, it is difficult to discern the solution structure of $[Fe(SR)_4]^-$ complexes with monodentate ligands. A case for the $S_4$ arrangement of the thiolate ligands about the metal center can be made due to observation that $S_4$ symmetry is the most stable conformation of many $R_4M$ compounds,[38] as well as the observation of this symmetry in four out of five of our structurally characterized $[Fe(SR)_4]^-$ complexes in the solid state. The simplicity and similarity of the spectra of the complexes containing monodentate thiolates may indicate that a $S_4$ structure is approached in solution. The distortions of the $[FeS_4]$ cores in these complexes could be expected to relax to a $T_d$ structure.

**$^1$H NMR Spectroscopy.** The $^1$H NMR spectrum of $[Fe(SPh)_4]^-$ in $CH_3CN$ has a resonance downfield at 60.4 ppm that is assigned to the meta hydrogens of the phenyl ring and two upfield resonances at –67.4 and –79.4 ppm that correspond to the ortho and para hydrogens. These resonances have significantly larger shifts than those of the Fe(II) compound that are at 22.3 ppm (*m*-H) and at –16.8 (*o*-H) and –23.5 ppm (*p*-H).[6] The change in sign and lack of attenuation of the chemical shifts in $[Fe(SPh)_4]^-$ are evidence of the dominant contribution of the contact interaction to the chemical shifts. The dominance of the contact versus dipolar shifts is a common feature of Fe–S compounds.[39,40] The larger shift in the Fe(III) compound results from its higher magnetic moment.

The $^1$H NMR spectrum of $[(n\text{-}Pr)_4N][Fe(SEt)_4]$ shows a ligand resonance at 49.0 ppm downfield from TMS. $[Ph_4P][Fe(S\text{-}i\text{-}Pr)_4]$ also shows only a single shifted resonance at 64.4 ppm. No shifted $^1$H resonance could be observed for $[Et_4N][Fe(SMe)_4]$. These results can be explained if the hydrogens on the $\alpha$-carbons are not being observed. The observed resonances are thus assigned to the $\beta$-methyl groups of the $SCH_2CH_3$ and $SCH(CH_3)_2$ ligands.

(36) Lovenberg, W.; Sobel, B. E. *Proc. Natl. Acad. Sci. U.S.A.* **1965**, *54*, 193–199.
(37) Eaton, W. A.; Lovenberg, W. In *Iron-Sulfur Proteins*; Lovenberg, W., Ed.; Academic Press: New York, 1973; Vol. II, Chapter 3.
(38) Karipides, A.; Iroff, L. D.; Mislow, K. *Inorg. Chem.* **1979**, *18*, 907–908. Narasimhamurthy, N.; Manohar, H.; Samuelson, A. G.; Chandrasekhar, J. *J. Am. Chem. Soc.* **1990**, *112*, 2937.
(39) Reynolds, J. G.; Laskowski, E. J.; Holm, R. H. *J. Am. Chem. Soc.* **1978**, *100*, 5315–5322.
(40) Hagen, K. S.; Watson, A. D.; Holm, R. H. *J. Am. Chem. Soc.* **1983**, *105*, 3905–3913.

**Table VII.** Redox Potentials for Rubredoxins and Synthetic Analogs

| compound | $E_{1/2}$, V vs SCE |
|---|---|
| $[Ph_4P][Fe(SPh)_4]$ | −0.50 (−0.52)[a] |
| $[Et_4N][Fe(SMe)_4]$ | −0.98 |
| $[(n\text{-}Pr)_4N][Fe(SEt)_4]$ | −1.07 (−1.08)[a] |
| $[Ph_4P][Fe(S\text{-}i\text{-}Pr)_4]$ | −1.11 |
| $[Et_4N][Fe(S\text{-}2,3,5,6\text{-}Me_4C_6H)_4]$ | −0.85 |
| $[Ph_4P][Fe(S\text{-}2,4,6\text{-}i\text{-}Pr_3C_6H_2)_4]$ | −1.10 |
| $[Et_4N][FeS_2\text{-}o\text{-}xyl)_2]$[2,3] | −1.03 |
| Rd (*Desulfovibrio acetoxidans*)[47] | −0.29 (1) |
| Rd (*Desulfovibrio salexignes*)[47] | −0.27 (1) |
| Rd (*Desulfovibrio gigas*)[47] | −0.24 (1) |
| Rd (*Clostridium pasteurianum*)[36] | −0.30 (2) |
| Rd (2Fe) (*Pseudomonas oleovorans*)[48] | −0.28 |
| desulforedoxin (*Desulfovibrio gigas*)[49] | −0.28 (2) |
| Fe(II) + Z-Cys-Pro-Leu-Cys-OMe (10% aqueous Triton X-100)[46] | −0.37 |
| $[Et_4N][FeS_2\text{-}o\text{-}xyl)_2]$ (10% aqueous Triton X-100)[46] | −0.64 |

[a] Reported value for the $[Fe^{II}(SR)_4]^{2-}$ compound.[7,40]

The resonances for the Fe(II) compound $[Fe^{II}(SEt)_4]^{2-}$ occur at +10.6 ppm ($-CH_3$) and +196 ppm ($-CH_2-$).[40] The shifts for the $\beta$-hydrogens in $[Fe^{III}(SEt)_4]^-$ are more than 4 times greater than those for the corresponding protons in the Fe(II) compound. It can be anticipated that the $\alpha$-hydrogens in the $[Fe^{III}(SR)_4]^-$ compounds will have downfield shifts that are again substantially greater than those for the corresponding Fe(II) compounds and thus could not be detected. It is noted that the $SCH_2-$ resonances in $[Fe_3S_4(SEt)_4]^{3-}$ also were not detected.[40]

$^1H$ NMR studies of oxidized and reduced rubredoxin have been performed by Phillips[41] and more recently by Markley.[42] In neither study were resonances with large shifts observed. Our results would suggest that the resonances for $SCH_2CH-$ protons of the coordinated cysteine residues in $Rd_{ox}$ were not observed in those studies. Recent studies by Kurtz of reduced Rd have located the $SCH_2-$ proton resonances that were not found in the earlier studies.[43] The $^1H$ NMR spectrum of $Rd_{ox}$ also should be reexamined in the region of 40–70 ppm downfield in an attempt to locate the methine protons of the cysteine ligands.

**Electrochemistry.** The redox potentials observed for $[Fe(SEt)_4]^-$ and $[Fe(SPh)_4]^-$ are in good agreement with the values of this couple measured previously for their Fe(II) analogs (Table VII).[6,40] The trend in the Fe(III)/Fe(II) couples reflects the differences in the electron-donating properties of the various thiolate ligands. $[Fe(SPh)_4]^-$ has the least negative potential, consistent with the electron-withdrawing properties of the phenyl group. The addition of electron-donating substituents in the ortho and para positions in $[Fe(S\text{-}2,3,5,6\text{-}Me_4C_6H)_4]^-$ and $[Fe(S\text{-}2,4,6\text{-}i\text{-}Pr_3C_6H_2)_4]^-$ results in a shift of the potentials to more negative values. The redox couple of $[Fe(SPh)_4]^-$ is reversible, as established by the superposition of the pulse and reverse-pulse polarographic waves. Similar electrochemical studies of $[Fe(S\text{-}2,3,5,6\text{-}Me_4C_6H)_4]^-$ and $[Fe(S\text{-}2,4,6\text{-}i\text{-}Pr_3C_6H_2)_4]^-$ indicate only quasi-reversible behavior of the 1−/2− couple. Although the reason for the irreversibility for the latter two compounds has not been determined, it may reflect the instability of their $[Fe^{II}(SR)_4]^{2-}$ complexes toward ligand dissociation. Both members of the $[Fe(SPh)_4]^{2-/-}$ redox couples have been characterized in the solid state and in solution. Although no Fe(II) complexes with the sterically hindered thiolate ligands have been prepared, $[Co^{II}(S\text{-}2,3,5,6\text{-}Me_4C_6H)_4]^{2-}$ has been characterized.[44] Unless excess thiolate is present in solution, the $[Co^{II}(S\text{-}2,3,5,6\text{-}Me_4C_6H)_4]^{2-}$ compound dissociates in acetonitrile solution to give $[Co(S\text{-}2,3,5,6\text{-}Me_4C_6H)_3(CH_3CN)]^- + RS^-$; an analogous behavior is apparently not displayed by the $[Co(SPh)_4]^{2-}$ complex.

The reduction potentials for the alkanethiolate complexes are very negative, indicating the ability of the electron-donating alkyl groups to stabilize the Fe(III) redox level. The shifts in the redox couple as a function of the alkanethiolates reflect the trend in the electron-donating properties of $-CH(CH_3)_2 > -CH_2CH_3 > -CH_3$. The large difference between the redox potentials of the $[Fe(S\text{–}alkyl)_4]^-$ analogs and that of the protein was previously noted for $[Fe(S_2\text{-}o\text{-}xyl)_2]^-$.[2,3] Similar differences have also been observed for redox levels of 2Fe- and 4Fe-S proteins measured in water and the redox levels of their inorganic synthetic analogs measured in aprotic solvents.[45] Studies of $[Fe(S_2\text{-}o\text{-}xyl)_2]^{2-}$ and an Fe(II) peptide complex in aqueous (10% Triton X100) solution have given potentials that were close to those of the biological compounds.[46–49]

**Summary and Conclusions.** A new and general synthetic route has allowed the synthesis and characterization of a wide range of $[Fe(SR)_4]^-$ complexes. This synthetic route has permitted the characterization of compounds that were previously thought to be too unstable with respect to oligomerization reactions and/or autoredox reactions to allow their isolation. This work provides another example in which it has been possible via synthetic inorganic chemistry to reproduce a biological metal center. The structures of three $[Fe(SR)_4]^-$ (R = Me, Et, Ph) complexes have been determined in the solid state. The structural analysis of $[M(SPh)_4]^{2-}$ complexes introduced by Coucouvanis has been extended and generalized to include the structure of $[Fe(SPh)_4]^-$. The tetragonal distortions in the $[MS_4]$ cores in $[M(SPh)_4]^{n-}$ compounds, which result from the intramolecular interactions between the PhS ligands and the $[MS_4]$ core, are determined by the symmetry of the $[M(SPh)_4]^{n-}$ anion.

**Acknowledgment.** This research was supported by NIH Grants GM 31849 and GM 36308. We thank J. Lauher for the use of his molecular graphics programs and T. O'Sullivan for assistance with the electrochemical measurements.

**Supplementary Material Available:** Listings of positional and thermal parameters for **1–3** and bond distances and angles, least-squares planes, and structural parameters for **3** (10 pages). Ordering information is given on any current masthead page.

(41) Phillips, W. D.; Poe, M.; Weiher, J. F.; McDonald, C. C.; Lovenberg, W. *Nature (London)* **1970**, *227*, 574–577.
(42) Krishnamoorthi, R.; Markley, J. L.; Cusanovich, M. A.; Przysiecki, C. T. *Biochemistry* **1986**, *25*, 50–54.
(43) Werth, M. T.; Kurtz, D. M.; Moura, I.; LeGall, J. *J. Am. Chem. Soc.* **1987**, *109*, 273.
(44) Koch, S. A.; Fikar, R.; Millar, M.; O'Sullivan, T. *Inorg. Chem.* **1984**, *23*, 121.
(45) Berg, J. M.; Holm, R. H. In *Iron-Sulfur Proteins*; Spiro, T. G., Ed.; Wiley: New York, 1982; Vol. IV, Chapter 1.
(46) (a) Nakata, M.; Ueyama, N.; Fuji, M.-A.; Nakamura, A.; Wada, K. Matsubara, H. *Biochim. Biophys. Acta* **1984**, *788*, 306–312. (b) Ueyama, N.; Nakata, M.; Fuji, M.-A.; Terakawa, T.; Nakamura, A. *Inorg. Chem.* **1985**, *24*, 2190–2196.
(47) Moura, I.; Moura, J. J. G.; Santos, M. H.; Xavier, A. V.; LeGall, J. *FEBS Lett.* **1979**, *107*, 419.
(48) Peterson, J. A.; Coon, M. J. *J. Biol. Chem.* **1968**, *243*, 329.
(49) Moura, I.; Huynh, B. H.; Hausinger, R. P.; LeGall, J.; Xavier, A. V.; Münck, E. *J. Biol. Chem.* **1980**, *255*, 2493–2498.
(50) Choudhury, S.; Dance, I. G.; Guerney, P. J.; Rae, A. D. *Inorg. Chim. Acta* **1983**, *70*, 227.
(51) Fukui, K.; Ohya-Nishiguchi, H.; Hirota, N. *Bull. Chem. Soc. Jpn.* **1991**, *64*, 1205.